FACTORS AFFECTING LATERAL STABILITY AND CONTROLLABILITY

By John P. Campbell and Thomas A. Toll

Langley Memorial Aeronautical Laboratory

The problem of obtaining satisfactory lateral stability has become increasingly difficult as airspeeds have increased and as designers have resorted to the use of extreme sweepback and low aspect ratio. At high speeds, many of our military airplanes have exhibited a lightly damped yawing oscillation – the so-called "snaking" oscillation. At low speeds, lateral-stability troubles are anticipated with sweptback and low-aspect-ratio designs, partly because of their relatively high effective dihedral and low damping in roll. In general, the problem of oscillatory, or Dutch-roll, stability does not now appear to be as serious for swept airplanes as originally anticipated, but in many cases it is important. In some cases, lateral controllability is a more important factor than Dutch-roll stability in determining the configuration of the airplane.

This paper will deal first with the effect on stability of some of the more important aerodynamic and mass characteristics and will then present methods for estimating the various stability parameters to be used in stability calculations for high-speed airplanes.

Two of the most important factors affecting lateral stability and controllability are the directional-stability parameter C_{n_β} (or C_{n_ψ}) and the effective-dihedral parameter C_{l_β} (or C_{l_ψ}). (See references 1 to 3.) These two factors are used as the basis for the conventional stability chart shown in figure 1. The ordinate is C_{n_β} and the abscissa is $-C_{l_\beta}$ which is positive effective dihedral. The boundary shown is for neutral oscillatory or Dutch-roll stability calculated for a general research model tested in the Langley free-flight tunnel. In the figure are two points which represent two models or airplanes with different combinations of C_{n_β} and C_{l_β}. The first point at high C_{n_β} and low C_{l_β} is for a good flying condition. The oscillatory stability is very good and the controllability is also good because the large value of C_{n_β} keeps adverse yawing to a minimum. The second point which has large C_{l_β} and low C_{n_β} represents a poor flying condition. It can be seen that since this point is below the stability boundary, Dutch-roll instability is indicated. Even if the boundary were below this point (which is quite likely in many cases) the controllability for this condition would be poor because the low directional stability would permit excessive adverse yawing, which in combination with the high effective dihedral will cause a serious reduction in aileron rolling

effectiveness. (See reference 4.) This happened in the case of the L-39 sweptback research airplane.

Another important factor affecting lateral stability is the damping in roll which becomes smaller as the sweepback is increased and as the aspect ratio is decreased. The effect on lateral stability of reducing the damping in roll is shown in figure 2 which is a stability chart similar to that already presented. The oscillatory-stability boundaries have been plotted for values of the damping-in-roll parameter C_{l_p} of 0, -0.1, and -0.2. The value of C_{l_p} for a straight wing conventional airplane is about -0.4 or -0.5. These boundaries which were taken from reference 5 were calculated for a hypothetical transonic airplane and are intended only to indicate the trends obtained as C_{l_p} is varied. It is evident from the boundaries that reducing C_{l_p} reduces lateral stability.

Several airplanes now in the design stage have provisions for variable wing incidence to permit the fuselage to remain at a low angle of attack while the wing goes up to the high angles of attack required because of the high sweep and low aspect ratio. Recent theoretical work (reference 6) which has been checked by tests in the Langley free-flight tunnel (reference 4) has indicated that increasing the wing incidence might have a detrimental effect on lateral stability. This effect is illustrated in figure 3, which is a stability chart for a free-flight-tunnel sweptback-wing model with 0° and 10° wing incidence.

Changing the wing incidence in effect changes the inclination of the principal axes of inertia of the airplane which is the factor that produces the change in stability. For example, in the case of the airplane with 0° wing incidence the fuselage is at the same angle of attack as the wing; and, because the principal longitudinal axis of inertia is usually approximately in line with the fuselage, it also has the same positive angle of attack. In the case of the wing with 10° wing incidence, however, it can be seen that the fuselage and, hence, the principal axes of inertia will have very little angle of attack. A comparison of the two boundaries shows that the effect of using positive wing incidence is to decrease the oscillatory stability. It therefore appears desirable to avoid the use of large positive wing incidence if possible. Some calculations have shown that even a small change in wing incidence (as small as 2°) can give large changes in stability.

The effects of mass distribution and relative density on lateral stability have been investigated both theoretically and by tests in the Langley free-flight tunnel (references 5, 7, and 8.) In general, the results have indicated that usually no pronounced effects on stability occur when the relative density is increased by increasing either the

wing loading or the altitude. Similarly, increasing the moment of inertia in yaw by increasing the weight in the fuselage does not usually appear to affect stability greatly. Increasing the moment of inertia in roll by increasing the weight carried in the wing, however, does have a pronounced effect on the stability as illustrated by figure 4, which is a stability chart for a typical sweptback fighter model tested in the Langley free-flight tunnel with and without wing tip tanks. A comparison of the two points on the chart shows that adding the tanks caused some slight changes in aerodynamic characteristics, but the main effect of the tanks was to increase the moment of inertia in roll which resulted in the large shift shown in the oscillatory-stability boundary. A pronounced reduction in the stability of the model is indicated when the wing tanks are installed. Since the period of the oscillation in this case is fairly long, however, it is possible that the airplane pilot would have less difficulty in flying with this unstable condition than he would in other cases where the oscillation is of shorter period and lightly damped.

Examples of lightly-damped short-period oscillations which are difficult to control have been encountered recently on a number of military airplanes. These airplanes exhibited poor lateral-oscillation characteristics or "snaking" in high-speed flight. A study of this snaking oscillation was recently conducted with a conventional single-engine low-wing attack airplane for which poor lateral-oscillation characteristics had been reported. The results of this investigation are summarized on figures 5 and 6. Figure 5 shows a time history of the rudder motion and yawing velocity after a disturbance in yaw for various rudder conditions for an indicated airspeed of about 350 miles per hour. With the rudder free, the snaking oscillation was very lightly damped even though the actual rudder deflections were less than half a degree. With the rudder locked the damping was much better and was considered satisfactory. The middle record shows that with just the rudder pedals fixed a true rudder-fixed condition was not obtained and the damping was not much better than with rudder free.

The variation of the damping with airspeed is shown in the first part of figure 6. The cycles required to damp to one-half amplitude and period of the oscillation are plotted as a function of indicated airspeed. With rudder locked, the damping in cycles remained constant over the speed range; while with rudder free with the original horn balance the damping was not as good as with rudder fixed at low speed and became progressively worse with increasing airspeed. When the horn balance was removed, the damping was essentially the same as with rudder locked.

An explanation for these changes in damping is given on the rudder-free stability chart on the right of this figure. On this plot of C_{n_ψ} against C_{n_δ} the calculated rudder-free stability boundaries for this

airplane with the effects of friction in the control system are taken into account. The boundaries, which were calculated by methods that were developed in references 9 and 10 and checked in reference 11, indicate the combinations of C_{h_ψ} and C_{h_δ} which produce stability, divergence, constant-amplitude oscillations, or increasing oscillations. With the horn balance the measured hinge-moment factors were as indicated by the point on the chart. The fact that this point is not far from the constant-amplitude oscillation boundary explains why at low speeds the damping was less with rudder free than with rudder fixed.

The decrease in damping with increase in airspeed for the rudder-free condition is attributed to the effects of Mach number on the hinge-moment parameters C_{h_ψ} and C_{h_δ}. Tests have shown that as Mach number is increased, both C_{h_ψ} and C_{h_δ} might become more positive which would shift the point on the chart towards a region of worse damping. Removing the horn balance makes both C_{h_ψ} and C_{h_δ} more negative and, therefore, shifts the point on the chart to a region of greater damping of the oscillation. This explains the improvement noted in the flight tests when the horn balance was removed. The current trend of airplane design which leads to intentional selection of a low C_{h_δ} and a positive C_{h_ψ} is such as to invite snaking or poorly damped oscillations. It is therefore important that the damping characteristics be checked by calculations and that due allowance be made for the effect of Mach number on the hinge-moment parameters.

Although the rudder hinge-moment characteristics appear to have a very important effect on snaking oscillations, other factors are undoubtedly involved in many cases. For example, fuel sloshing has in some cases appeared to make the snaking motion worse, and such factors as the air flow at the tail-fuselage juncture and the arrangement of the tail pipe in the fuselage have been shown to affect snaking. Even when none of these factors are involved, an airplane might exhibit snaking in the rudder-fixed condition just because the damping of the Dutch-roll oscillation is weak. This might be the reason for the snaking experienced with the XS-1. The fact that in high-speed flight, the fuselage (and thus the principal longitudinal axis of inertia) is more nearly alined with the relative wind will tend to make the Dutch-roll oscillation damping worse than at low speeds.

The discussion presented so far has indicated some of the design conditions that must be avoided if satisfactory lateral stability characteristics are to be obtained. In general, it has been found through experience with models in the Langley free-flight tunnel that flight characteristics can be predicted through solutions of the equations of motion, provided sufficient information is at hand regarding

the mass characteristics of the models and the values of the stability derivatives.

The theoretical stability derivatives given for unswept wings in reference 12 have generally been found to be adequate. The use of sweep may affect the values of some of the derivatives appreciably however; and, in general, the available rigorous theories applicable to swept wings are too cumbersome to be used for the preparation of charts similar to those given for unswept wings in reference 12. Analyses of swept-wing data, such as those given in reference 13, have indicated that through simple geometric considerations, correction factors may be derived to account for the effects of sweep. When these factors are applied to rigorous theoretical values of the derivatives of unswept wings, reasonably reliable derivatives for swept wings may be obtained. Such factors have been derived for the various derivatives and are given in reference 14. Some sample charts based on the method of reference 14 are shown in figure 7. These charts illustrate trends resulting from the effects of sweep on some of the important stability derivatives of wings having a taper ratio of 0.5 and no dihedral.

Perhaps the greatest effect of sweep is on the effective-dihedral derivative $-C_{l_\beta}$. It should be noted that for small aspect ratios, a given angle of sweepback may result in high positive effective dihedral; whereas, the same angle of sweepforward may result in little or no negative effective dihedral. This is caused by the fact that, although the increment of C_{l_β} resulting from sweep does not vary to any large extent with aspect ratio, the value of $-C_{l_\beta}$ for unswept wings increases rapidly as the aspect ratio decreases.

The approximate method of calculation indicates that the damping in roll C_{l_p} is reduced by sweep, but this effect generally is not large except for relatively high aspect ratios. In this connection, it might be mentioned that the effectiveness of ailerons, which occupy a given portion of the wing surface, is found to decrease with sweep more rapidly than the damping in roll. If it is desired, therefore, to meet the usual rolling criterion of a specified value of the wing-tip helix angle $\frac{pb}{2V}$, either larger ailerons or greater deflections must be provided as the sweep angle is increased.

Sweep causes appreciable increases in the magnitudes of the derivatives of yawing moment due to rolling C_{n_p} and rolling moment due to yawing C_{l_r}. This is in contrast to the reductions noted for the value of C_{l_p} and usually found for the lift-curve slope C_{L_α}.

Experimental determinations of the various stability derivatives have been made for a large number of wings through the use of the rolling- and curved-flow equipment of the Langley stability tunnel. In general, the test results have substantiated the trends shown by the charts. The data have indicated, however, that under some conditions, the calculated values of the derivatives may apply to only a limited lift-coefficient range. This fact is illustrated by figure 8 which shows comparisons of experimental and calculated values of the derivatives $-C_{l_\beta}$, C_{l_r}, and C_{n_p} for an untapered 45° sweptback wing of aspect ratio 2.6. The tests, which were made at a Reynolds number of about 1,400,000, are reported in references 15 and 16.

For this case, the initial slopes of the derivatives against lift coefficient are in fairly good agreement with the slopes indicated by the calculations. The data begin to deviate from the initial slopes, however, at a lift coefficient of about 0.5, and the deviations become very important at high lift coefficients. Under these test conditions, the rolling moment due to sideslip and the rolling moment due to yawing decreased to about zero at maximum lift. The yawing moment due to rolling reversed its sign at a lift coefficient of about 0.7, so that at high lift coefficients the derivative C_{n_p} might be regarded as favorable rather than unfavorable as is normally expected. This can have an important effect on controllability at high lift coefficients. Free-flight-tunnel tests of models with positive values of C_{n_p} have indicated that the favorable yaw makes it possible to obtain good lateral flying characteristics without the necessity of coordinating the rudder with aileron control.

The deviations of the experimental data from the initial slopes probably result from tip stalling since rolling- and yawing-moment derivatives are affected primarily by flow conditions at the tips. An indication of partial stalling is given by the rise in the quantity $C_D - \frac{C_L^2}{\pi A}$ which represents that part of the wing drag which is not ideally associated with lift. For convenience, this quantity will be referred to as the "drag index." For the case of a sweptback wing without devices which tend to delay stalling at the wing tips, such as vanes, leading-edge flaps, or slots, the drag index is found to rise at about the lift coefficient at which the derivatives C_{l_β}, C_{l_r}, and C_{n_p} begin to deviate from the trends established at low lift coefficients. When devices which delay tip stalling are used, the drag index may not be a true indication of variations in derivatives, however, for it may rise because of separation of flow from inboard parts of the wing which would not greatly affect the rolling- and yawing-moment derivatives. For plain sweptback wings, however, it appears that the drag index might serve as a basis for predicting the lift-coefficient range over which the calculated characteristics might be expected to apply under specific conditions. An

important application of the drag-index concept is in the prediction of Reynolds number effects on derivatives such as C_{n_p} and C_{l_r} which can be determined only with special equipment which normally is not available in wind tunnels capable of making tests at high Reynolds numbers.

Figure 9 shows the effects of Reynolds number and of wing roughness on the effective-dihedral derivative $-C_{l_\beta}$ and on the drag index for a 40° sweptback wing with an NACA 64_1-112 airfoil section. These results, taken from reference 17, are from tests made in the Langley 19-foot pressure tunnel. Large effects of Reynolds number were noted when the wing surface was smooth; for example, at a Reynolds number of 5,300,000, the derivative $-C_{l_\beta}$ increased linearly with lift coefficient almost until maximum lift was attained, and the drag index showed very little change with lift coefficient. At a Reynolds number of 1,720,000, however, the derivative $-C_{l_\beta}$ began to deviate from its initial trend at a lift coefficient of about 0.5, and the drag index showed an abrupt rise at the same lift coefficient. Results obtained at a high Reynolds number, for the wing with roughness at the leading edge, were very similar to results obtained at a low Reynolds number for the wing with a smooth surface. The drag index again indicates the presence of tip stalling for the latter two cases but little or no stalling for the smooth wing at a high Reynolds number. It might be expected therefore that initial trends of the derivatives C_{n_p} and C_{l_r} also would persist to a high lift coefficient for the case of the smooth wing at a high Reynolds number.

The shape of the wing profile may, under some conditions, have large effects on lateral stability characteristics. Figure 10 shows comparisons of results obtained on the effective dihedral derivative $-C_{l_\beta}$ for smooth wings having NACA 64_1-112 and circular-arc airfoil sections. The tests (reference 18) were made at a Reynolds number of 5,300,000, which is the higher of the two values referred to in the preceding figure. With flaps off, the curve for the NACA 64_1-112 airfoil is the same as given before. The values of $-C_{l_\beta}$ for the circular-arc airfoil begin to deviate from their initial trend at a very low lift coefficient, probably because the tendency of sweptback wings to stall at the tips is aggravated through the use of an airfoil with a sharp leading edge. With leading-edge and trailing-edge flaps deflected, the derivative $-C_{l_\beta}$ continued to increase almost linearly with lift coefficient until maximum lift was approached, regardless of the airfoil section. It appears that the wing characteristics are determined largely by the contour of the leading-edge flap and that the basic airfoil section has very little influence when the leading-edge flap is deflected. Since the leading-edge flap tends to delay tip stalling, it is probable that the

derivatives C_{n_p} and C_{l_r} also would show trends similar to that indicated for $-C_{l_\beta}$.

The discussion given so far has dealt largely with the more important effects of sweep on characteristics that are of particular interest at low speeds. In the design of a complete airplane, additional factors, such as the effects of the fuselage, or the size and location of the tail surfaces, must be considered. Experience has indicated that the effects of these additional factors on the various rotary-stability derivatives and on the effective-dihedral derivative $-C_{l_\beta}$ can be accounted for in much the same manner that has been used for conventional-aircraft designs. Particular attention should be paid, however, to the possible adverse effect of swept wings on directional stability near maximum lift. It is not yet possible to select with any degree of certainty a configuration that will have satisfactory directional stability characteristics at all lift coefficients, but it generally has been possible to correct an undesirable condition in the course of wind-tunnel development tests.

Very little theoretical or experimental information regarding subsonic compressibility effects on the lateral-stability derivatives is available at the present time. Results of tests made on one model in the Langley high-speed 7- by 10-foot tunnel are shown in figure 11. The tests included determinations of the derivatives C_{n_β}, $-C_{l_\beta}$, and C_{l_p} through a range of Mach number. The model configuration used in the determination of C_{l_p} was slightly different from that used in the determinations of C_{n_β} and $-C_{l_\beta}$. The compressibility effects on these derivatives were found to be very small for Mach numbers below 0.82. At higher Mach numbers, the directional-stability derivative C_{n_β} increased, probably because, with the model in sideslip, the critical Mach number of the leading-wing panel was exceeded and, consequently, the drag of the leading-wing panel increased. At an angle of attack of 6° the effective-dihedral derivative $-C_{l_\beta}$ decreased as the Mach number exceeded 0.82. This probably results from a loss in lift on the leading-wing panel as its critical Mach number is exceeded. The damping-in-roll derivative C_{l_p} showed no abrupt change through the test range of Mach number.

The problem of lateral behavior at transonic speeds, extending through a Mach number of 1.0, is now being investigated by means of free-flight rocket models, but results are not yet available. Several theoretical investigations which apply to Mach numbers of about 1.2 and above have been completed or are in progress. The case of the supersonic derivatives of triangular wings already has been covered rather completely in reference 19. The methods used in reference 19 are now

being extended to "notched" triangles, or swept wings with zero taper ratio. Investigations of unswept rectangular wings also are underway.

In summarizing, it might be said that progress is being made in the determination of the stability derivatives for swept and low-aspect-ratio airplane configurations; and it appears that by using the proper stability derivatives with existing theoretical methods, the lateral stability characteristics of high-speed airplanes can, at least qualitatively, be predicted.

[redacted]

REFERENCES

1. McKinney, Marion O., Jr. : Experimental Determination of the Effects of Dihedral, Vertical-Tail Area, and Lift Coefficient on Lateral Stability and Control Characteristics. NACA TN No. 1094, 1946.

2. Drake, Hubert M. : The Effect of Lateral Area on the Lateral Stability and Control Characteristics of an Airplane as Determined by Tests of a Model in the Langley Free-Flight Tunnel. NACA ARR No. L5L05, 1946.

3. Drake, Hubert M. : Experimental Determination of the Effects of Directional Stability and Rotary Damping in Yaw on Lateral Stability and Control Characteristics. NACA TN No. 1104, 1946.

4. McKinney, Marion O., Jr. and Drake, Hubert M. : Correlation of Experimental and Calculated Effects of Product of Inertia on Lateral Stability. NACA TN No. 1370, 1947.

5. Sternfield, Leonard : Some Considerations of the Lateral Stability of High-Speed Aircraft. NACA TN No. 1282, 1947.

6. Sternfield, Leonard : Effect of Product of Inertia on Lateral Stability. NACA TN No. 1193, 1947.

7. Campbell, John P., and Seacord, Charles L., Jr. : The Effect of Mass Distribution on the Lateral Stability and Control Characteristics of an Airplane as Determined by Tests of a Model in the Free-Flight Tunnel. NACA Rep. No. 769, 1943.

8. Campbell, John P., and Seacord, Charles L., Jr. : Effect of Wing Loading and Altitude on Lateral Stability and Control Characteristics of an Airplane as Determined by Tests of a Model in the Free-Flight Tunnel. NACA ARR No. 3F25, 1943.

9. Greenberg, Harry, and Sternfield, Leonard : A Theoretical Investigation of the Lateral Oscillations of an Airplane with Free Rudder with Special Reference to the Effect of Friction. NACA Rep. No. 762, 1943.

10. Neumark, S. : A Simplified Theory of the Lateral Oscillations of an Aeroplane with Rudder Free, Including the Effect of Friction in the Control System. Rep. No. Aero 2049, British R.A.E., May 1945.

11. Maggin, Bernard : Experimental Verification of the Rudder-Free Stability Theory for an Airplane Model Equipped with a Rudder Having Positive Floating Tendencies and Various Amounts of Friction. NACA TN No. 1359, 1947.

[redacted]

12. Pearson, Henry A., and Jones, Robert T. : Theoretical Stability and Control Characteristics of Wings with Various Amounts of Taper and Twist. NACA Rep. No. 635, 1938.

13. Letko, William, and Goodman, Alex : Preliminary Wind-Tunnel Investigation at Low Speed of Stability and Control Characteristics of Swept-Back Wings. NACA TN No. 1046, 1946.

14. Toll, Thomas A., and Queijo, M. J. : Approximate Relations and Charts for the Low-Speed Stability Derivatives of Swept Wings. (Prospective NACA paper)

15. Feigenbaum, David, and Goodman, Alex: Preliminary Investigation at Low Speeds of Swept Wings in Rolling Flow. NACA RM No. L7E09, 1947.

16. Goodman, Alex, and Feigenbaum, David: Preliminary Investigation at Low Speeds of Swept Wings in Yawing Flow. NACA RM No. L7I09, 1947.

17. Neeley, Robert H., and Conner, D. William: Aerodynamic Characteristics of a 42° Swept-Back Wing with Aspect Ratio 4 and NACA 64_1-112 Airfoil Sections at Reynolds Numbers from 1,700,000 to 9,500,000. NACA RM No. L7D14, 1947.

18. Salmi, Reino J., and Fitzpatrick, James E.: Yaw Characteristics and Sidewash Angles of a 42° Sweptback Circular-Arc Wing with a Fuselage and with Leading-Edge and Split Flaps at a Reynolds Number of 5,300,000. NACA RM No. L7I30, 1947.

19. Ribner, Herbert S., and Malvestuto, Frank S., Jr. : Stability Derivatives of Triangular Wings at Supersonic Speeds. (Prospective NACA paper)

Campbell

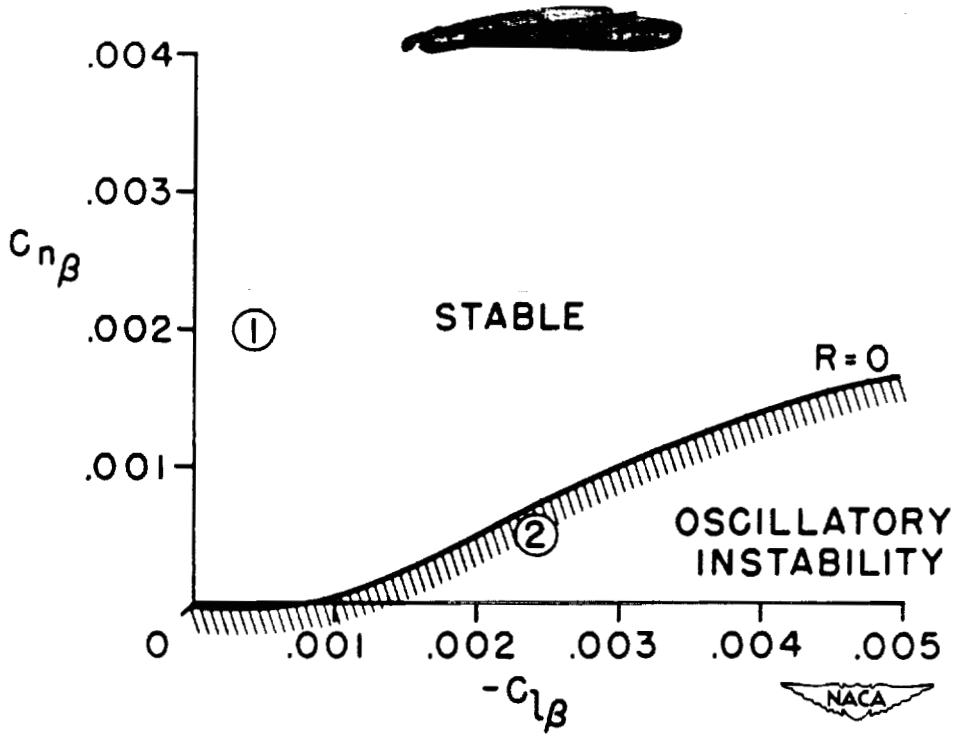

Figure 1.- Stability chart for a general research model tested in the Langley free-flight tunnel (C_L = 1.0).

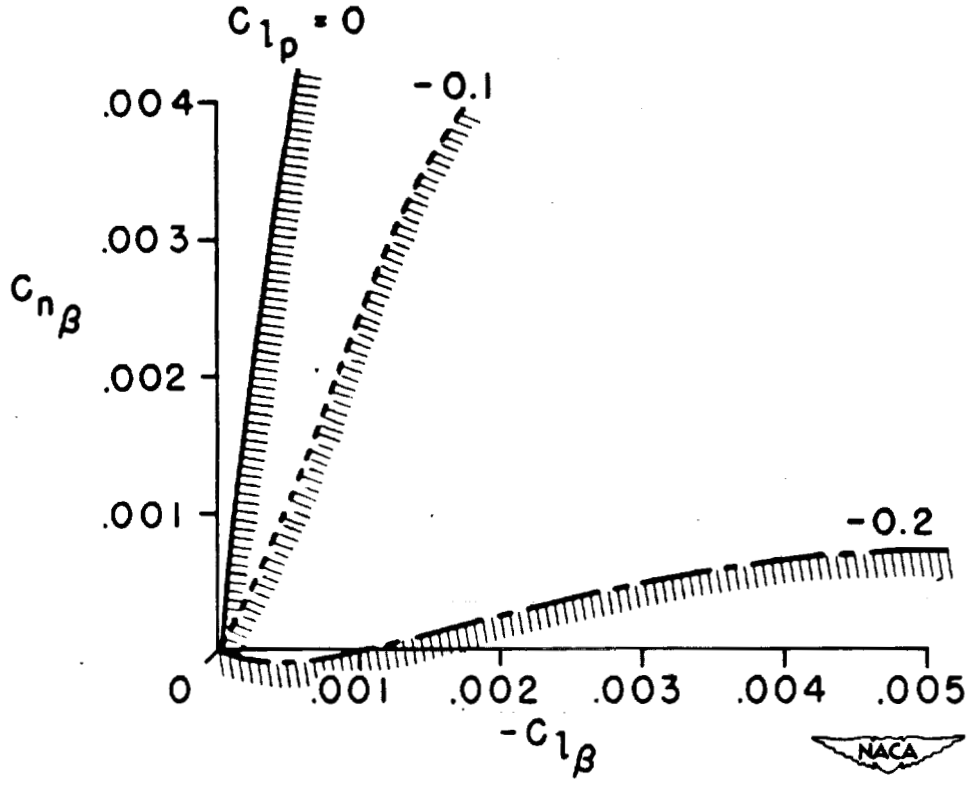

Figure 2.- Effect of damping in roll on the lateral stability of a high-i airplane (C_L = 1.0).

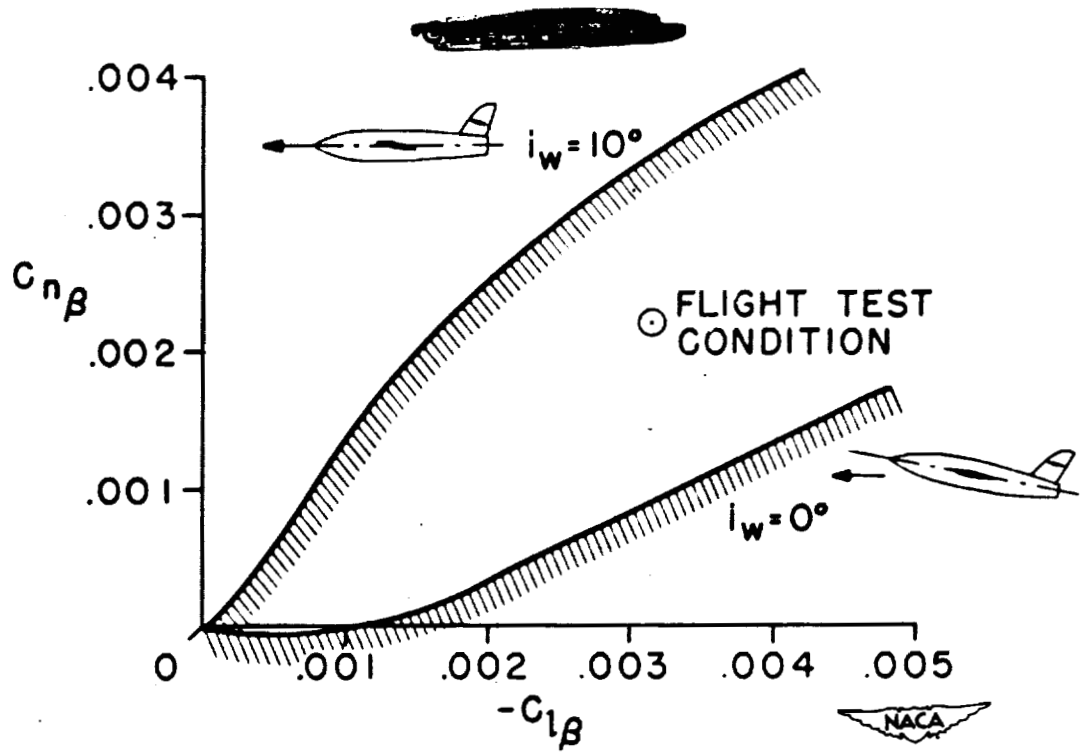

Figure 3.- Effect of wing incidence on the lateral stability of a free-flight-tunnel research model (C_L = 0.6).

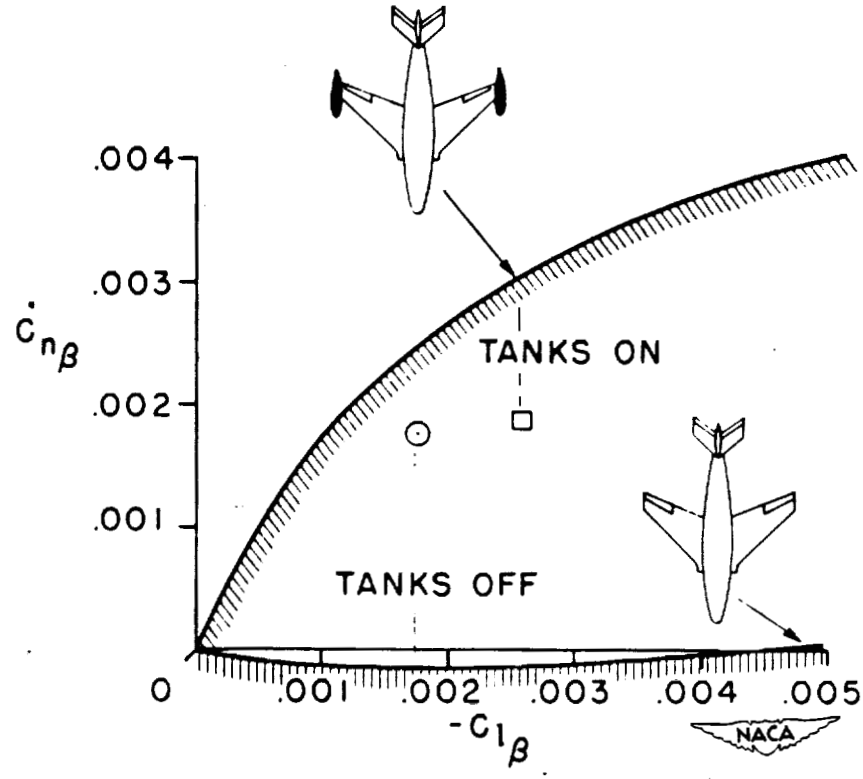

Figure 4.- Effect on the lateral stability of the change in mass distribution caused by adding wing-tip tanks (C_L = 0.7).

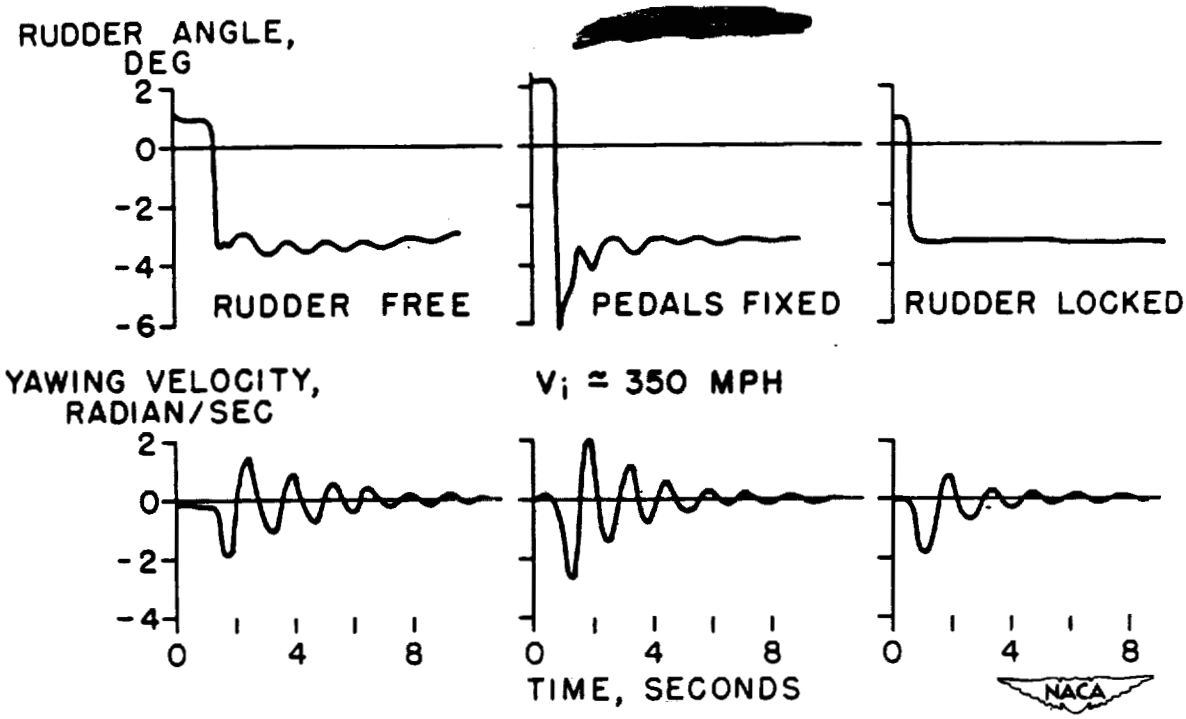

Figure 5.- Time histories of the lateral oscillations of a conventional attack airplane.

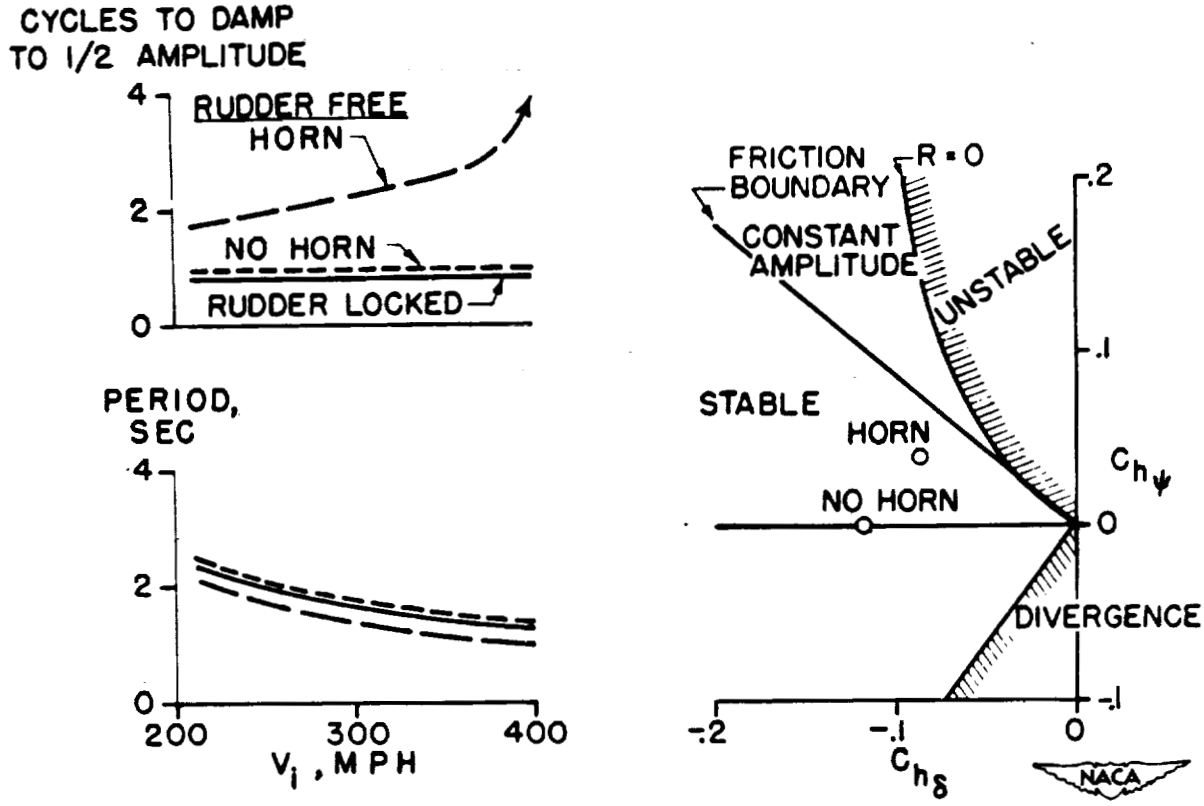

Figure 6.- Period and damping of the lateral oscillation and calculated rudder-free stability boundary for conventional attack airplane.

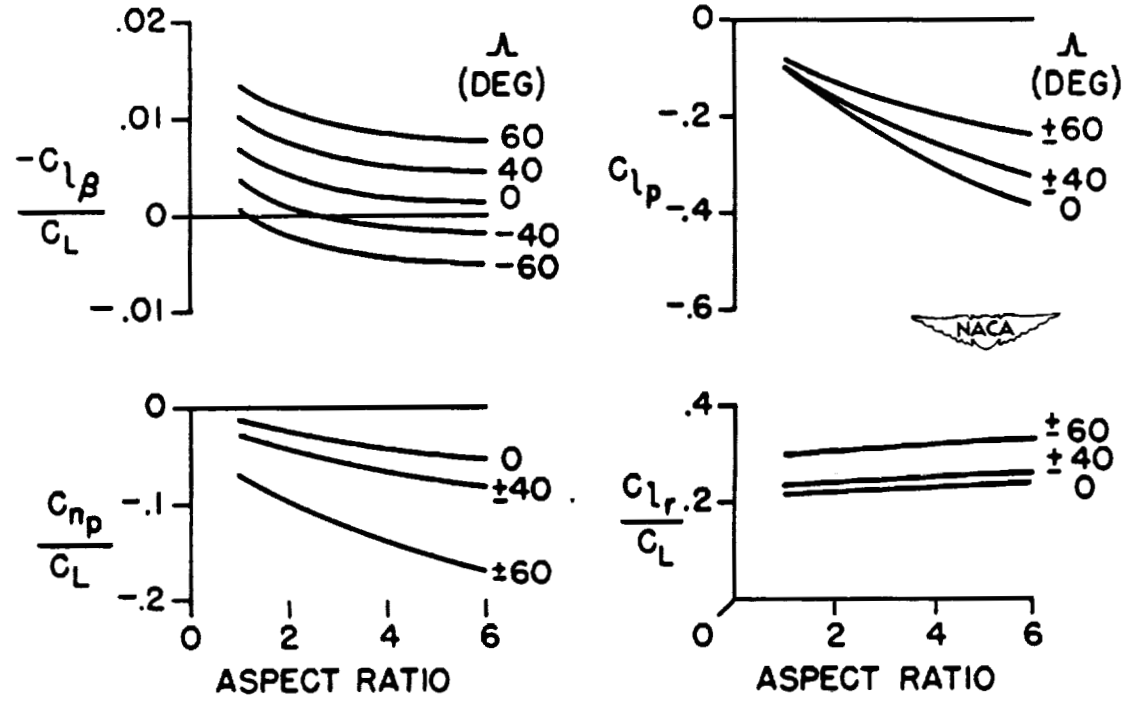

Figure 7.- Lateral-stability derivatives calculated by approximate theory for swept wings with taper ratio of 0.5.

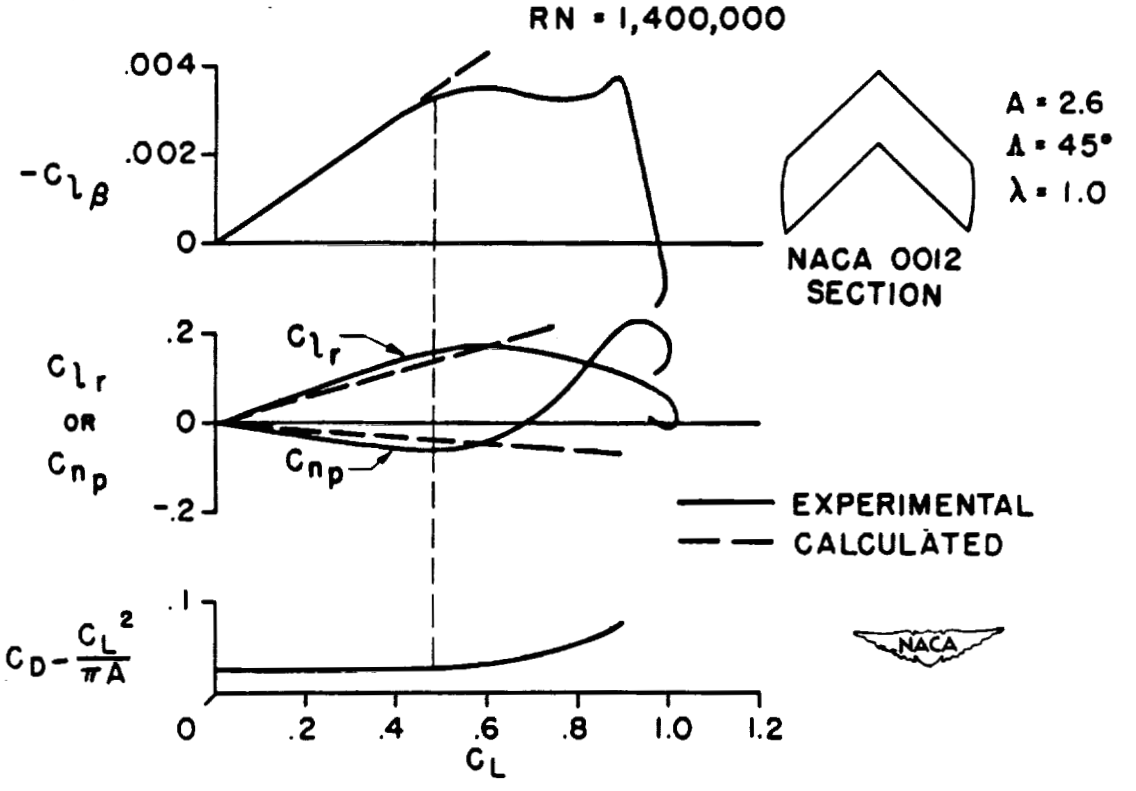

Figure 8.- Comparison of experimental and calculated lateral-stability derivatives.

Campbell

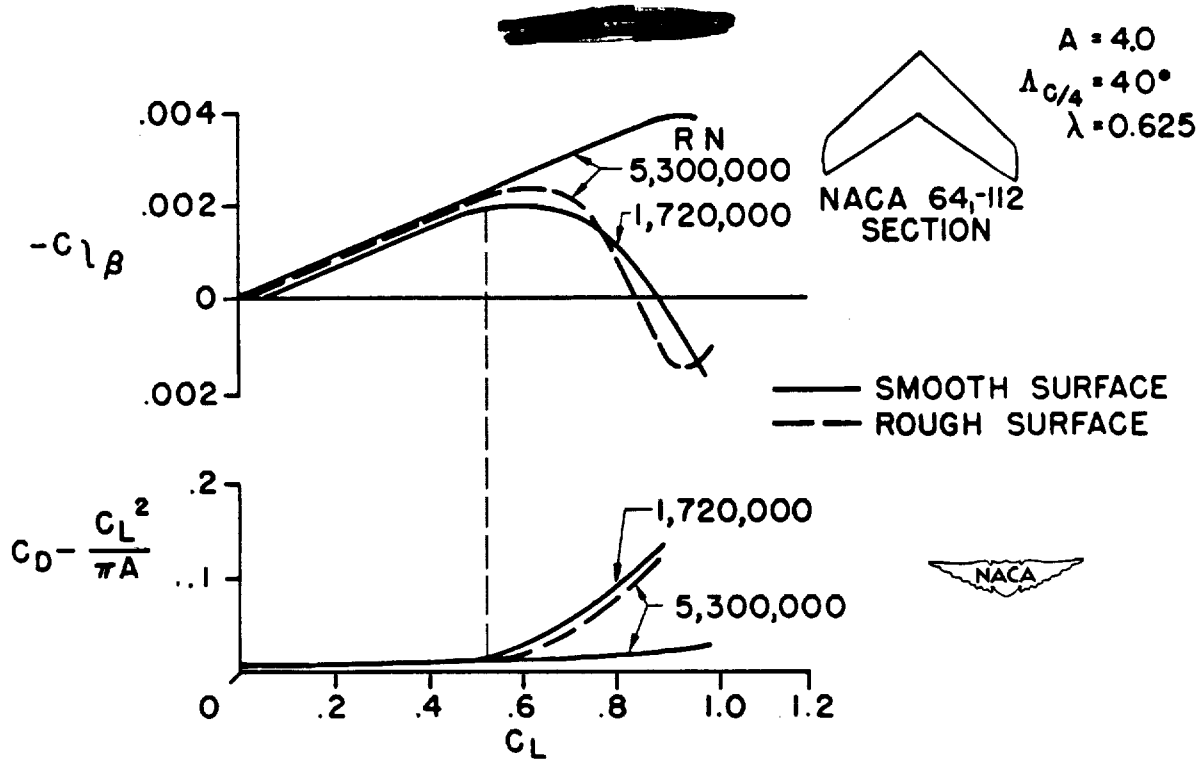

Figure 9.- Effect of Reynolds number and wing roughness on rolling moment due to sideslip.

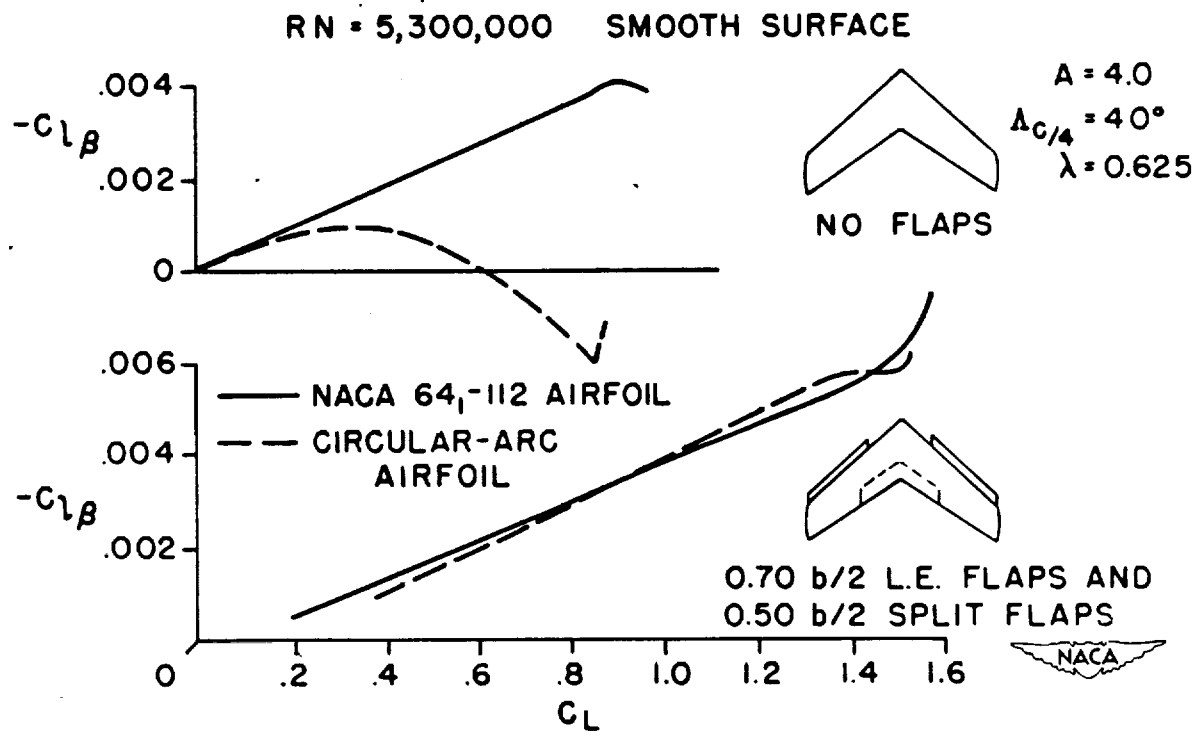

Figure 10.- Effect of airfoil section and flaps on rolling moment due to sideslip.

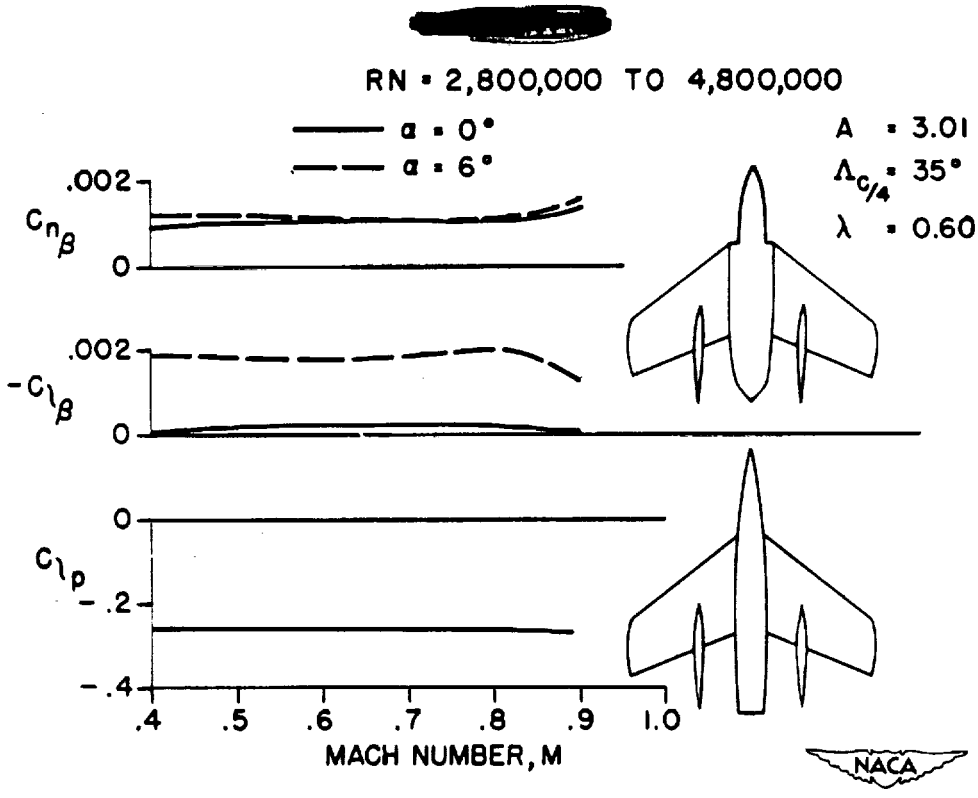

Figure 11.- Effect of Mach number on lateral-stability derivatives.